$^{40}Ar/^{39}Ar$ geochronology of submarine Mauna Loa volcano, Hawaii

Brian R. Jicha[1*], J. Michael Rhodes[2], Brad S. Singer[1], Michael O. Garcia[3]

[1] *Department of Geoscience, University of Wisconsin, Madison, Wisconsin, 53706, USA*

[2] *Department of Geosciences, University of Massachusetts, Amherst, Massachusetts, 01003, USA*

[3] *Department of Geology & Geophysics, University of Hawaii, Honolulu, Hawaii, 96822, USA*

*Email: bjicha@geology.wisc.edu

Abstract

New geochronologic constraints refine the growth history of Mauna Loa volcano and enhance interpretations of the petrologic, geochemical, and isotopic evolution of Hawaiian magmatism. We report results of $^{40}Ar/^{39}Ar$ incremental heating experiments on low-K, tholeiitic lavas from the 1.6 km high Kahuku landslide scarp cutting Mauna Loa's submarine southwest rift zone, and from lavas in a deeper section of the rift. Obtaining precise $^{40}Ar/^{39}Ar$ ages from young, tholeiitic lavas containing only 0.2-0.3 wt.% K_2O is challenging due to their extremely low radiogenic ^{40}Ar contents. Analyses of groundmass from 45 lavas yield 14 new age determinations (31% success rate) with plateau and isochron ages that agree with stratigraphic constraints. Lavas collected from a 1250 m thick section in the landslide scarp headwall were all erupted around 470 ± 10 ka, implying an extraordinary period of accumulation of ~25 mm/yr, possibly correlating with the peak of the shield-building stage. This rate is three times higher than the estimated vertical lava accumulation rate for shield-building at Mauna Kea (8.6 ± 3.1

mm/yr) based on results from the Hawaii Scientific Drilling Project. Between ~470 and 273 ka, the lava accumulation rate along the southwest rift zone decreased dramatically to ~1 mm/yr. We propose that the marked reduction in lava accumulation rate does not mark the onset of post-shield volcanism as previously suggested, but rather indicates the upward migration of the magma system as Mauna Loa evolved from a submarine stage of growth to one that is predominantly subaerial, thereby cutting off supply to the distal rift zone. Prior to ~250 ka, lavas with Loihi-like isotopic signatures were erupted along with lavas having typical Mauna Loa values, implying greater heterogeneity in the plume source earlier in Mauna Loa's growth. In addition to refining accumulation rates and the isotopic evolution of the lavas erupted along the southwest rift zone, our new ^{40}Ar/^{39}Ar results constrain the eruption of the Ninole Basalts from 227-108 ka and provide maximum estimates on the timing of the Ka Lae and South Kona landslides.

1. Introduction

A major impediment to our understanding of the growth of Hawaiian volcanoes, and therefore the nature and structure of the Hawaiian plume, has been a lack of thick stratigraphic sections from which to obtain long temporal records of magmatic history. The older volcanoes in the Hawaiian Island chain (< 7 Ma) are deeply weathered, commonly mantled by alkalic post-shield lavas, and have subsided into the Pacific Ocean, all of which obscure the more voluminous, shield-building record [*Macdonald and Abbott*, 1970]. The protracted eruptive histories of younger active volcanoes, such as Mauna Loa, are buried by recent flows [*Lockwood and Lipman*, 1987]. Radiocarbon dating of charcoal beneath Mauna Loa subaerial lavas has produced a detailed eruptive chronology that spans only the last 35 ka [*Lockwood,* 1995; *Trusdell and Lockwood*, in press]. The older eruptive record of Mauna Loa is poorly documented by K-Ar data, which are imprecise and provide spuriously old ages due to excess ^{40}Ar [*Dalrymple and Moore,* 1968; *Lipman et al.*, 1990; *Lipman,* 1995].

The Hawaii Scientific Drilling Project (HSDP) made significant advancement towards documenting the long-term magmatic evolution of adjacent Mauna Kea volcano. *Sharp and Renne* [2005] utilized the ^{40}Ar/^{39}Ar incremental heating method, which has a distinct advantage over conventional K-Ar methods in that it can identify whether a sample has been subject to post-crystallization potassium loss/addition or if it has retained excess argon—two problems that plague geochronology of Hawaiian tholeiites [*Dalrymple and Moore,* 1968; *Renne*, 2000]. Their ^{40}Ar/^{39}Ar-based age model for HSDP-2 indicates that the 3.1 km core records more than 400 ka of Mauna Kea's magmatic history. These lavas are overlain by a 246 m veneer of young (< 122 ka) Mauna Loa lavas [*Sharp et al.*, 1996; *Sharp and Renne,* 2005]. *Sharp and Renne* [2005] determined that building of the submarine to subaerial flank of Mauna Kea tholeiitic shield volcano took place at a mean rate of 8.6 ± 3.1 mm/y, whereas post-shield subaerial lavas accumulated at a much lower rate of only 0.9 ± 0.4 mm/y. The dramatic decrease in accumulation rate occurred rather abruptly at ~330 ka, which coincided with a transition in lava composition from exclusively tholeiitic basalts to transitional and alkali basalts inter-layered with tholeiitic basalts [*Rhodes and Vollinger*, 2004].

To evaluate comparable long-term magmatic history of Mauna Loa volcano we conducted an ^{40}Ar/^{39}Ar investigation on a stratigraphically controlled sample suite that was collected from three vertical transects of the 1.6 km high Kahuku landslide scarp cut into Mauna Loa's submarine southwest rift zone using Pisces V and Jason submersibles (Figure 1)[Garcia et al., 1995]. The new ^{40}Ar/^{39}Ar ages are consistent with stratigraphy in all cases and indicate a very rapid period of magma accumulation (~ 25 mm/y) at ~470 ka followed by waning activity

(< 1 mm/y) from ~400 to 59 ka. In addition, we report new $^{40}Ar/^{39}Ar$ ages for dredged samples from: (1) the toe of the submarine southwest rift zone in an attempt to expand Mauna Loa's magmatic history, (2) a dredged sample of the South Kona debris avalanche on the southwest submarine flank of the volcano in order to place maximum limits on the age of the avalanche event, and (3) a subaerial lava flow and dike from the Ninole Basalts to place firmer age constraints on these enigmatic lavas (Figure 1).

2. Geologic setting and sample description

2.1 Mauna Loa and the southwest rift zone

Mauna Loa is the largest active volcano on Earth rising more than 8000 m above the Cretaceous Pacific Ocean floor. Most of its eruptive activity has been from the large summit caldera and along two prominent rift zones that trend northeast and southwest from the summit [*Lockwood and Lipman*, 1987]. The northeast rift zone extends for ~40 km before it is buried by younger Kilauea lavas. The southwest rift zone is 103 km long, of which 33 km are below sea level, descending to a depth of 4500 m (Figure 1). Giant landslides have dissected Mauna Loa's submarine flanks including the southwest rift zone [e.g., *Lipman et al.*, 1988; *Moore et al.*, 1989]. The Ka Lae landslide, one of the youngest on Mauna Loa, produced a 1.6 km high scarp that is the submarine extension of the prominent Kahuku scarp. This scarp exposes a "mile-high" section of pillow lavas cut by numerous thin (<1 m) dikes [*Garcia et al.*, 1995]. It is the thickest lava section exposed on any Hawaiian volcano. Lavas were collected from three vertical traverses of this section using the Pisces V submersible (dives 182-184) and Jason (dives 16, 19, and 20) in 1991 and 2002 respectively. Jason dives 23 and 24 sampled surface flows from a distal section of the southwest rift.

2.2 Ninole Basalt

The origin of the basaltic lavas exposed on the deeply eroded Ninole Hills on Mauna Loa's southern flank and their relation to Mauna Loa's southwest rift zone has been the subject of a long-lasting debate. They were considered to be the remnants of an older, pre-Mauna Loa volcano [*Stearns and Clark*, 1930; *Macdonald and Abbott*, 1970]. However, *Lipman et al.* [1990] suggest that the Ninole Basalts represent blocks of older Mauna Loa lavas that have slumped southward as a result of the Punaluu landslide. Their argument is based, in part, on the similarity in abundance and ratios of alteration resistant trace elements with young Mauna Loa lavas. They also note that the weighted mean K-Ar age is 120 ± 56 ka [*Lipman et al.*, 1990] for three basalts from the Ninole Hills supports an origin from Mauna Loa, but not an older volcano. *Morgan et al.* [2010] adopt the *Lipman et al.*, [1990] age estimate for the Ninole Basalts, but suggest that these lavas erupted from an earlier, north trending precursor to the southwest rift zone. $^{40}Ar/^{39}Ar$ experiments were undertaken on a basaltic lava and two dikes from Makanau Hill and Puu Enuhe [*Lipman et al.,* 1990] in an effort to more precisely constrain the age of the Ninole Basalts and evaluate these models.

2.3 South Kona and Ka Lae landslides

The South Kona debris avalanche is thought to be the oldest of the giant landslides that occurred on the western flank of Mauna Loa [*Moore et al.,* 1989; *Moore and Clague,* 1992]. This avalanche involved multiple failures that moved blocks, some >10 km in length, up to 80 km from the ancestral shoreline of Mauna Loa [*Moore et al.,* 1995]. The South Kona landslide is thought to be caused by at least two events generated by the oversteepening of accumulated volcanic material on the island [*Moore et al.,* 1995]. Initial failure leading to the major debris avalanche is estimated to have occurred after ~250 ka, about the time attributed to emergence of Mauna Loa above sea level. This assumption is primarily based on very imprecise K-Ar and $^{40}Ar/^{39}Ar$ ages [*Moore et al.,* 1995; *Lipman et al.,* 1995; *Morgan et al.,* 2007]. Two samples were chosen for $^{40}Ar/^{39}Ar$ geochronology from blocks within the South Kona deposits that were dredged in 1999 offshore from the constructional flanks of Mauna Loa. These samples provide a maximum age for this landslide.

Mauna Loa's southwest rift zone has distinct coastal benches that are capped by a coral reef that is currently 150 meters below sea level (mbsl) [*Moore et al.,* 1990]. U-Th ages and paleoenvironmental reconstructions suggest that the reef drowned ~14-15 ka [*Moore et al.,* 1990; *Webster et al.,* 2004]. Obtaining $^{40}Ar/^{39}Ar$ ages from near the top of the submarine Kahuku landslide scarp provide a maximum age limit for the timing of the Ka Lae landslide, whereas the published U/Th ages for the coral reef constrain the minimum age of the slide.

3. Potassium mobility

There is no evidence for thermally-activated diffusional loss of argon in lava samples from HSDP-1 and -2 cores [*Sharp and Renne,* 2005]. However, the lowermost 2000 m of the 3098 m HSDP-2 core sampled submarine flows and hyloclastites, where potassium mobility during low temperature alteration is a potential problem [*Sharp and Renne*, 2005]. Previous studies have shown that basalts tend to gain potassium if subject to seawater alteration at low temperature [*Staudigel et al.*, 1996]. If potassium gain occurs post-crystallization, $^{40}Ar/^{39}Ar$ ages of the altered groundmass will be younger than their true ages. Potassium loss due to interaction with meteoric water will have the opposite effect, resulting in older apparent $^{40}Ar/^{39}Ar$ ages [e.g., *Pringle*, 1993]. The ratio K_2O/P_2O_5 is a sensitive gauge of post-solidification potassium mobility in Hawaiian tholeiitic basalt because P_2O_5 is relatively immobile under conditions of submarine alteration [*Lipman et al.,* 1990; *Frey and Rhodes,* 1993]. *Rhodes and Vollinger* [2004] and *Stolper et al.* [2004] suggest that K_2O/P_2O_5 values of 1.4-1.7 and 1.5-1.8 are indicative of un-altered values for whole-rock and glass, respectively, in Hawaiian lava flows. All of the samples analyzed in this study have K_2O/P_2O_5 ratios between 1.4 and 1.9.

4. $^{40}Ar/^{39}Ar$ methods

$^{40}Ar/^{39}Ar$ incremental heating experiments were undertaken on 45 lavas from Mauna Loa, and two Mauna Kea lavas from the HSDP-2 drill core. Samples were crushed, sieved to 250-350 μm, and phenocrysts were removed via magnetic sorting or density separation using methylene iodide. The groundmass was treated with 3.5 N HCl in an ultrasonic bath, rinsed thoroughly, and then washed ultrasonically with deionized water twice. Additional ultrasonic cleaning of the groundmass was done in a 1M nitric acid solution followed by repeated cleaning in deionized water. Microphenocrysts that survived mechanical separation or groundmass which still showed evidence of alteration were removed by hand picking under a binocular microscope. Phenocryst-free, acid leached groundmass separates were weighed and then wrapped in 99.99% copper foil packets placed into in 2.5cm diameter aluminum disks with 28.201 Ma Fish Canyon tuff sanidine (FCs) [*Kuiper et al.*, 2008], which monitors neutron fluence. Up to six aluminum disks were assembled into a cylindrical stack and irradiated at the Oregon State University TRIGA-type reactor in the Cadmium-Lined In-Core Irradiation Tube (CLICIT). Six different irradiations spanning 1.5 to 4 hours were performed over a three year period. The irradiation parameter J was determined for each sample by analyzing ~10-12 grains of FCs at different positions within an aluminum disk.

At the University of Wisconsin-Madison Rare Gas Geochronology Laboratory, ~ 200 mg groundmass packets were incrementally heated in a double-vacuum resistance furnace attached to a 300 cm^3 gas clean-up line. Prior to sample introduction, furnace blanks were measured at 100 °C increments throughout the temperature range spanned by the incremental heating experiment and interpolated. Blanks were less than 2×10^{-16}, 2×10^{-19}, 2×10^{-19}, and 7×10^{-19} moles for ^{40}Ar, ^{39}Ar, ^{37}Ar, ^{36}Ar, respectively. Following blank analyses, samples were degassed at 550 °C for 60 to 75 minutes to potentially remove large amounts of atmospheric argon. Experiments consisted of 7-16 steps from 600-1350 °C; each step included a two-minute increase to the desired temperature, which was maintained for 15 minutes, followed by an additional 15 minutes for gas cleanup. The gas was cleaned during and after the heating period with three SAES C50 getters, two of which were operated at ~450 °C and the other at room temperature. Argon isotope analyses were done using a MAP 215-50 mass spectrometer using a single Balzers SEM-217 electron multiplier, and the isotopic data was reduced using ArArCalc software version 2.5 (http://earthref.org/ArArCALC/).

The single most important parameter when obtaining $^{40}Ar/^{39}Ar$ age determinations for low-K tholeiites with low concentrations of radiogenic ^{40}Ar is quantification of the mass-dependent bias that is introduced during ionization of the sample gas in the mass spectrometer source. This correction is commonly referred to as the mass discrimination correction and is determined by measuring the isotopic composition of purified atmospheric argon with an automated pipette system. Atmospheric argon was measured 6–10 times prior to, and following each furnace incremental heating experiment. Quantities of atmospheric argon are typically $1x10^{-14}$ moles for ^{40}Ar, but were varied at times throughout the analytical sessions to encompass the range of ^{40}Ar observed for sample unknowns. No dependence on mass discrimination with air aliquot size was observed. Measured $^{40}Ar/^{36}Ar$ ratios of atmospheric argon were normalized to $^{40}Ar/^{36}Ar = 295.5$ [*Steiger and Jäger,* 1977] and the discrimination was calculated using a power law relationship [*Renne et al.,* 2009].

Because of the low ^{40}Ar radiogenic yields and thus imprecise ages obtained for these young Mauna Loa lavas, replicate (up to 5) experiments were performed on all of the samples to improve precision. The age uncertainties reported in Table 1 reflect analytical contributions only at the 2σ level; the decay constants used are those of *Min et al.* [2000]. Our criteria for an acceptable plateau are similar to those outlined by *Sharp and Renne* [2005]; a plateau must include: (1) three or more consecutive steps that contain $\geq 60\%$ of the ^{39}Ar released, (2) have a probability of fit of at least 0.05, and (3) have no resolvable slope. We also exclude data from weighted mean plateau age and isochron calculations that have an analytical uncertainty $\geq$ 10X that of the sample's most precise step, thereby preventing inflation of the probability of fit [*Sharp and Renne*, 2005].

5. $^{40}Ar/^{39}Ar$ results

Groundmass separated from 45 Mauna Loa lavas yields 14 new age determinations, which translates to a 31% success rate. Approximately 80% of the failed samples have age spectra that form a staircase upward pattern with ages typically exceeding 1.5 Ma in the higher temperature steps. This pattern is characteristic of samples being contaminated with excess argon. The remainder of the failed samples contained little (<0.5%) or no radiogenic ^{40}Ar. We were unable to identify a geochemical or mineralogical indicator that could be used to distinguish the successful vs. unsuccessful samples. However, it should be noted that most of the failed samples had total K/Ca ratios of < 0.03 and larger than expected ^{38}Ar signals, which may be Cl-derived. Moreover, no $^{40}Ar/^{39}Ar$ ages were obtained from samples with bulk rock K_2O contents of < 0.3 wt.%.

Results from 38 incremental heating experiments on the 14 samples that gave meaningful ages and the two HSDP-2 samples are summarized in Table 1. Complete analytical data are available in online supplementary material. All samples that define statistically acceptable plateaus have isochrons with trapped $^{40}Ar/^{36}Ar$ ratios that are indistinguishable from the atmospheric $^{40}Ar/^{36}Ar$ ratio of 295.5. For this reason coupled with the observation that each $^{40}Ar/^{39}Ar$ age is consistent with its stratigraphic position, we consider the plateau ages to give the best estimate of the time elapsed since eruption (Table 1). Our results contrast with those of *Sharp and Renne* [2005] who found that 12 of 14 Mauna Kea tholeiites had trapped $^{40}Ar/^{36}Ar$ ratios ranging from 298-306 with the submarine tholeiites having the most variability. The origin of this difference is unknown. However, the preferred ages obtained for two HSDP-2 core samples (one subaerial and one submarine) analyzed in both laboratories are indistinguishable (see below).

5.1 Inter-laboratory comparison of Mauna Kea tholeiites from HSDP-2

The Hawaii Scientific drilling project recovered core samples from a ~3-km-deep drill hole that penetrates shield lavas of both Mauna Loa and Mauna Kea volcanoes [*DePaolo et al.,* 1999; *Garcia et al.,* 2007]. Fourteen submarine and subaerial Mauna Kea tholeiites, one alkalic basalt in the upper ~140 km of the Mauna Kea section, and one Mauna Loa tholeiite were analyzed by *Sharp and Renne* [2005] using the $^{40}Ar/^{39}Ar$ incremental heating technique. We analyzed two of these Mauna Kea tholeiites, a subaerial lava (SR413-4.0) and a pillow lava (SR781-21.2), from the HSDP-2 drill core to assess inter-laboratory reproducibility and calibrate our results to those obtained for the core. Our two experiments each on samples SR413-4.0 and SR781-21.2 gave weighted mean plateau ages of 364 ± 93 and 488 ± 75 ka (Figure 2), respectively, which are indistinguishable from the preferred $^{40}Ar/^{39}Ar$ isochron ages of 372 ± 180 and 485 ± 67 ka of *Sharp and Renne* [2005] (the *Sharp and Renne* [2005] ages have been recalculated relative to 28.201 Ma for the Fish Canyon tuff sanidine; *Kuiper et al.* [2008]). The mean plateau ages of 392 ± 70 and 529 ± 55 ka obtained by *Sharp and Renne* [2005] for these samples are also indistinguishable from our weighted mean plateau ages.

5.2 Submarine southwest rift zone

The location of submarine samples collected along Mauna Loa's southwest rift zone by the Pisces V and Jason submersibles are shown in Figure 1. The submarine Kahuku landslide scarp was systematically sampled along three vertical sections, Pisces dives 182 and 183, Pisces Dive 184 in 1991 [*Garcia et al.,* 1995], and Jason dives 16, 19 and 20 in 2002. These three sections are roughly 3-4 km apart. The depth of these sample locations are shown schematically in Figure 3. In the subsequent discussion (and Table 1) we refer to the actual water depth (mbsl) and the depth below the top of the section. This is because we assume that the top of the section is roughly isochronous and that therefore the depth in section is a more reliable indicator of stratigraphic position than actual water depth of collection.

Sample J2-16-04 was collected from the stratigraphically deepest part (2112 mbsl, 1622 m in the section) of the Kahuku landslide scarp on the submarine southwest rift zone. Three incremental heating experiments yield plateaus that comprised ~90%, 96%, and 100% of the ^{39}Ar released and the corresponding plateau ages are in good agreement (Figure 4a). The weighted mean plateau age is 470 ± 74 ka (Table 1). In addition, if all of the data from the three experiments are regressed together, they define a 22-step isochron of 456 ± 144 ka, an initial $^{40}Ar/^{36}Ar$ ratio of 295.8 ± 2.8, and a Mean Square of Weighted Deviate (MSWD) of 0.22 (Figure 4b).

Multiple experiments from tholeiites higher in the section sampled by Jason and Pisces V dives at 1263, 650, 470, and 367 m deep in the section give largely concordant spectra (> 93% of ^{39}Ar released in all cases) with weighted mean plateau ages of 463 ± 28, 468 ± 38, and 461 ±

36 ka, respectively, all of which are indistinguishable from the 470 ± 74 ka lava at 1622 m in the section. Of these, Sample J2-20-14, located at 857 mbsl (367 m in the section), yields a weighted mean plateau age of 474 ± 27 ka, the most precise age determination in this study (± 6%), which is probably due to the higher radiogenic ^{40}Ar in this sample (5-11%) compared to other submarine Mauna Loa lavas (1-4%). The mean plateau age is indistinguishable from the other dated flows that are stratigraphically below. The degassing patterns of the two incremental heating experiments of J2-20-14 are nearly identical. The plateau steps are concordant for more than 75% of the initial ^{39}Ar released, but subsequent heating steps at high temperature have K/Ca ratios of 0.03-0.04 and give ages that are significantly older (up to 1.8 Ma) than the mean plateau age, suggesting that heterogeneous trapped excess or inherited ^{40}Ar may be present (Figure 5a, b).

Four ^{40}Ar/^{39}Ar ages were obtained from the upper 178 m of the section. Two analyses of sample J2-20-17 at a depth of 178 m in the section yield fully concordant plateaus with a weighted mean age of 273 ± 55 ka. These subsamples also yield a statistically acceptable combined isochron with an age of 212 ± 96 ka and an initial ^{40}Ar/^{36}Ar ratio of 297.4 ± 3.4 (Table 1). Sample J2-20-20, a tholeiite with 0.67 wt.% K_2O at 110 m in section, was analyzed three times, yielding two fully concordant plateaus and one with a plateau comprising 99.6% of the ^{39}Ar released (Figure 6a). The weighted mean age based on the three experiments is 196 ± 12 ka. The combined isochron gives an age of 144 ± 47 ka and a trapped ^{40}Ar/^{36}Ar ratio of 299.1 ± 4.9 (Figure 6b). The high temperature steps of each experiment, although imprecise, are slightly older than the mean age suggesting that a minor amount of excess or inherited ^{40}Ar may be present in this sample. Pisces V sample 184-13 from 550 mbsl (top of Pisces 184 section) is the highest dated flow clearly identified within the landslide scarp. Two experiments on this sample gave an imprecise age of 120 ± 43 ka, which is in agreement with the stratigraphy of the section.

Sample J2-20-22 from 501 mbsl was collected from a relatively flat area above the landslide scarp, and may well be a surface flow. It has a K_2O/P_2O_5 ratio of 1.25, indicating some potassium loss. Two experiments give plateau ages of 55 ± 24 and 62 ± 23 ka (weighted mean = 59 ± 16 ka), a combined isochron age of 52 ± 35 ka, an initial $^{40}Ar/^{36}Ar$ ratio of 296.6 ± 6.5 (Figure 7). The two other nearby samples collected beyond sample J2-20-22 are unsuitable $^{40}Ar/^{39}Ar$ dating. Therefore, we are unable to evaluate to what degree potassium loss has affected sample J2-20-22.

5.3 Surface flows from the deepest southwest rift zone

Two samples from Jason dive 24 (Figure 1) were dated from the deepest part of the southwest rift zone (3963 and 4537 mbsl) in an effort to expand our knowledge of Mauna Loa's earliest magmatic history. An olivine-phyric basalt from 3963 mbsl, J2-24-14, was analyzed twice and gave a weighted mean plateau age of 543 ± 150 ka. Two experiments from J2-24-01, the deepest lava flow collected at 4537 mbsl, yielded plateau ages of 856 ± 209 and 637 ± 108 ka (Figure 8a). The weighted mean plateau age based on these two experiments is 683 ± 96 ka, but the MSWD is 3.5 owing to the disparity between the two plateau ages. The 637 ka subsample is significantly more precise because it has an average radiogenic ^{40}Ar yield of 3.5% compared to 2.1% for the 856 ka subsample. The combined 15-step isochron defines an age of 657 ± 175 ka with a MSWD of 0.17 (Figure 8b). We prefer this more conservative estimate for the age of this sample given the disagreement between the two plateau ages. Another surface lava from the deepest part of the southwest rift zone, J2-25-01, was analyzed, but it yields a strongly discordant spectra with geologically unreasonable ages exceeding 3.4 Ma (not shown).

5.4 South Kona debris avalanche deposit

A fine-grained, basaltic block (M12-03) was dredged from the South Kona debris avalanche deposit ~20 km from the southwestern shore of Hawaii at a depth of 3700 mbsl (Fig. 1). A single experiment yielded a plateau that encompasses 87% of the ^{39}Ar released and defines an age of 247 ± 56 ka, an imprecise isochron age of 185 ± 147 ka, and an initial $^{40}Ar/^{36}Ar$ ratio of 301.6 ± 18.7 (Figure 9). The last three heating steps of the experiment produce ages that exceeded >850 ka, suggesting that excess ^{40}Ar may have been retained in high temperature microcrystalline phases (e.g., olivine, clinopyroxene, plagioclase) in the groundmass. Analysis of an additional subsample yielded a highly discordant age spectra with ages near 1.0 Ma (Figure 9), apparently reflecting sample heterogeneity. Multiple experiments on several of the Mauna Kea tholeiites analyzed by *Sharp and Renne* [2005] also gave both concordant and discordant spectra and were attributed to heterogeneous trapped excess ^{40}Ar.

5.5 Ninole Basalt

A basaltic lava flow and two dikes from the Ninole Basalts were analyzed to evaluate the ages of these subaerial Mauna Loa lavas. Based on whole-rock K-Ar dating, *Lipman et al.* [1990] indicate that "the best estimate for the age of the Ninole Basalt is 0.1-0.2 Ma, with an upper limit of 0.3 Ma". K-Ar analyses did not detect any radiogenic ^{40}Ar in basaltic lava SW-45, and a basaltic dike (SW-77) gave a spuriously old K-Ar age of 1.28 ± 0.80 Ma (2σ) [*Lipman et al.,* 1990]. However, two $^{40}Ar/^{39}Ar$ incremental heating experiments on purified groundmass, not whole rock powder which was used for the K-Ar analyses, from lava sample SW-45 gave concordant age plateaus that define ages of 211 ± 38 and 237 ± 29 ka. The weighted mean plateau age is 227 ± 23 ka and the combined 17-step isochron age is 232 ± 29 ka with a MSWD of 0.41 (Figure 10a,b). The dike sample SW-77 was analyzed twice and yields plateaus defined by 87% of the ^{39}Ar released that are in good agreement with a weighted mean age of 108 ± 35 ka (Figure 10). Another basaltic dike, sample SW-91, failed to yield detectable radiogenic ^{40}Ar. Overall, Ninole Basalts are constrained to have erupted between 227-108 ka.

6. Discussion

6.1 Ages of the South Kona and East Ka Lae landslides

Numerous submarine landslides reflecting massive gravitational failures of oversteepened volcano flanks were identified along the Hawaiian Chain following the GLORIA sidescan sonar surveys of the Hawaiian Exclusive Economic Zone [*Lipman et al.,* 1988; *Moore et al.,* 1989; *Moore et al.*, 1994]. Three major debris avalanches (South Kona, Alika 1, and Alika 2) and several smaller landslides (e.g., Ka Lae) have originated from the southwestern flanks of Mauna Loa volcano [*Lipman et al.*, 1988; *Moore et al.,* 1989]. Here we reassess the published ages for the South Kona and Ka Lae landslides and discuss how our new age data constrain the timing of these landslides.

The age of the South Kona debris avalanches are poorly known and are thought to have occurred around 250 ka [*Moore et al.*, 1989; *Lipman et al.,* 1988; *Moore et al.*, 1995]. Using the ^{230}Th excess dating technique, *McMurtry et al.* [1999] obtained an age of 240 ± 80 ka for a turbidite layer in ODP site 842, ~300 km west of Mauna Loa, that is interpreted to be associated with the South Kona debris avalanche. Our ^{40}Ar/^{39}Ar age of 247 ± 56 ka from a basaltic block within the debris avalanche, together with the turbidite age of 240 ± 80 ka [*McMurty et al.*, 1999], provide the most reliable constraints on the timing of South Kona landslide.

The East Ka Lae debris avalanche on the southwest submarine flank of Mauna Loa is interpreted to be younger than the Alika 1, Alika 2, and South Kona landslides because of its more rugged appearance in the GLORIA sonograms [*Moore and Clague*, 1992], and because the

Ka Lae scarp cuts into the remnants of the South Kona landslide [*Moore and Chadwick*, 1995]. The East Ka Lae landslide exposes a > 1.6 km section of pillow lavas in Mauna Loa's southwest rift zone, which are the focus of this study. The youngest dated pillow lava sampled from the landslide scarp (Pisces 184-13) with an age of 120 ± 43 ka provides a maximum age for the East Ka Lae landslide. Support for this maximum age is provided by large rounded boulders, relicts of a former shoreline, perched at the edge of the landslide scarp at a depth of 425 mbsl [*Garcia et al.*, 1995]. We find it implausible that these boulders could have been stably deposited at the edge of the landslide scarp during active shoreline development. Therefore, we conclude that this former shoreline was truncated by the landslide. Based on coastal subsidence curves for the island of Hawaii, incorporating both isostatic subsidence rates (~ 2.5 mm/y) with changes in sea level [*Moore et al.*, 1990] we infer that this former shoreline formed around 130 ka, indicating that the landslide is even younger.

A well-developed, submerged coral reef is located 150 mbsl off South Point, stratigraphically above the landslide scarp (Figure 3). The reef has grown on a bench that is the continuation of Mauna Loa's subaerial slope. At about 160 m there is a distinct break in slope, suggestive of a former shoreline [*Moore et al.*, 1990; *Garcia et al.*, 1995]. A coastal subsidence curve indicates an age of 16–30 ka for this old shoreline [*Moore et al.*, 1990]. Most importantly, this break in slope is not observed to the west of the landslide scarp [*Garcia et al.*, 1995] implying that it may have been truncated by the landslide. Therefore, the East Ka Lae debris avalanche likely occurred sometime between 120 and 30 ka.

6.2. Age Constraints on the Isotopic Composition of Mauna Loa Magmas

Subaerial Mauna Loa lavas are compositionally and isotopically distinct from lavas of neighboring Kilauea, Mauna Kea and Loihi volcanoes [e.g., *Wright*, 1971; *Garcia et al.*, 1989;

Frey and Rhodes, 1993; *DePaolo et al.,* 2001]. Some older submarine Mauna Loa lavas, however, have major element compositions similar to young subaerial lavas, but with isotopic (e.g. Pb, Sr, Nd and He) and trace element ratios (e.g. Zr/Nb, La/Yb, K/Nb) that overlap with those of neighboring volcanoes [e.g., *Garcia et al.,* 1995; *Kurz et al.,* 1995; *DePaolo et al., 2001*]. There is, however, a gradual decrease in $^{3}He/^{4}He$, $^{206}Pb/^{204}Pb$ and $^{143}Nd/^{144}Nd$ with a corresponding increase in $^{87}Sr/^{86}Sr$ with time [*Kurz et al.*, 1995]. These changes in isotopic and trace element ratios are generally attributed to heterogeneities in the plume source and the passage of Mauna Loa over either a concentrically zoned plume [e.g. *Kurz et al.*, 1995; *DePaolo et al.*, 2001], or one that is bilaterally asymmetrical [e.g. *Abouchami et al.*, 2005; *Weis et al.,* 2011].

Extensive isotopic data (Pb, Sr, Nd, Hf) exists for Mauna Loa lavas, ranging in age from historical (1843 -1984) eruptions to the submarine lavas at the base of the Mile High section (>470 ka) [*Weis et al.,* 2011]. Most, including the submarine lavas, are isotopically similar, and are characteristic of Mauna Loa. For example, Mauna Loa lavas cluster around 18.1 for $^{206}Pb/^{204}Pb$ and 37.9 for $^{208}Pb/^{204}Pb$, although some submarine lavas have Loihi-like Pb isotopic compositions with higher values of both $^{206}Pb/^{204}Pb$ and $^{208}Pb/^{204}Pb$ (Figure 11). Others have unusually high $^{208}Pb/^{204}Pb$ relative to $^{206}Pb/^{204}Pb$ compared with other Hawaiian shield lavas [*Weis et al.,* 2011]. Our data enable us to establish a time frame in which these heterogeneities appeared in Mauna Loa lavas. Sample M12-03, a 247 ± 56 ka dredge sample from the South Kona landslide, and two other South Kona landslide samples from dredges M12 and M13 have the highest $^{206}Pb/^{204}Pb$ ratios (up to 18.4) among Mauna Loa lavas, comparable with Loihi values. These results indicate that the plume source for Mauna Loa magmas was more heterogeneous earlier in the volcano's history. A Loihi-like component was therefore present in the source of Mauna Loa magmas prior to ~250 ka. Numerous samples with unusually high $^{208}Pb/^{204}Pb$ relative to $^{206}Pb/^{204}Pb$ are also found in both PISCES and JASON dives along the Kahuku submarine landslide scarp, and in submarine dredge samples from the southwest rift zone. All of these samples are at a depth of >680 m below the top of the scarp in the Mile High section, implying an age of >470 ka (Figures 3, 11). PISCES dive sample 184-7 is the shallowest sample in the section (690 m) with elevated $^{208}Pb/^{204}Pb$ relative to $^{206}Pb/^{204}Pb$. Above it, at 470 m, is a PISCES sample 184-8 with "normal" ratios of $^{208}Pb/^{204}Pb$ relative to $^{206}Pb/^{204}Pb$. It is dated at 461 ± 36 ka. Therefore, we conclude that lavas with elevated $^{208}Pb/^{204}Pb$ relative to $^{206}Pb/^{204}Pb$ were erupted prior to ~470 ka. Assuming Pacific Plate motion is ~10 cm/y to the northwest, Mauna Loa would have been located about 25 to 47 km to the southeast of its present position (roughly halfway between the present positions of Loihi and Mauna Loa) and was sampling more of these components in the plume than it is today.

6.3 Lava ccumulation rates for Mauna Loa

Detailed mapping of subaerial flows combined with ^{14}C dating of charcoal beneath the lavas provide high-resolution constraints on Mauna Loa's magmatic history for only the last 35 ka [*Lipman and Swenson, 1984;*; *Lockwood*, 1995; Wolf and Morris, 1996; *Trusdell and Lockwood*, in press]. Quantifying longer-term lava accumulation rates at Mauna Loa (and other Hawaiian volcanoes) has been hampered by the lack of thick, exposed sections as well as imprecise and inaccurate K-Ar ages [*Lipman*, 1995]. Using nine new $^{40}Ar/^{39}Ar$ ages (Table 1), we establish an age-depth profile for the 1.6 km section of pillow lavas from the submarine southwest rift zone exposed by the Ka Lae landslide (Figure 12), the longest section exposed on any Hawaiian volcano. The sequence is characterized by two distinct lava accumulation rates. From 1622 to 367 m depths in the section (2112 to 857 mbsl) lavas were emplaced during an extremely vigorous eruptive period at ~ 470 ka. The $^{40}Ar/^{39}Ar$ ages of upper and lowermost lavas in this 1255m thick sequence are indistinguishable. Using the minimum age defined by the uncertainty of the uppermost lava (474 ka -27 ka = 447 ka) and the maximum age for the lower lavas, which is controlled by the 463 ± 28 ka lava (463 ka + 28 ka = 491 ka), we calculate a minimum lava accumulation rate for this sequence of at least 25 mm/yr (see dotted line in Figure 12). This estimate is much higher than the 8–9 mm/yr found in HSDP-2 for the shield-building stage of Mauna Kea volcano [*Sharp and Renne*, 2005]. However, the HSDP-2 site is located >50 km away from Mauna Kea's summit and was deliberately located far (~ 20 km) from an inferred Mauna Kea east rift zone [*Stolper et al*, 1996]. Our ~25 mm/yr accumulation rate at ~ 470 ka is higher than the ~7 mm/yr accumulation rate for the southwest rift zone of Mauna Loa based on the model of *DePaolo et al*. [2001] (Figure 12), and it is only somewhat less than the 'peak' accumulation rates (50-35 mm/yr) proposed for an entire Hawaiian volcano [*DePaolo and Stolper*, 1996].

Between ~470 and 273 ka, the lava accumulation rate along the southwest rift zone decreased dramatically to ~1 mm/yr and it remained at this rate until at least 59 ka (Figure 12). These results verify previous suggestions that the rate of magma supply and lava accumulation along Mauna Loa's submarine southwest rift zone has declined dramatically over the last 200-300 ka [*Moore et al.*, 1990; *Lipman*, 1995], but our new data extend the period to much earlier time (> 400 ka). This decline in eruption rate was used to suggest Mauna Loa was nearing the end of shield volcanism [*Moore et al.* 1990] and that post-shield volcanism was imminent [*Lipman,* 1995]. HSDP-2 results indicate a similar dramatic decrease in accumulation rate occurred at Mauna Kea at about 330 ka (Figure 12), coinciding with the transition from exclusively tholeiitic shield basalts to a mixed sequence of tholeiitic, transitional tholeiitic, and alkali basalts during the post-shield stage [*Rhodes and Vollinger,* 2004; S*harp and Renne,* 2005].

Unlike Mauna Kea lavas in HSDP-2, Mauna Loa lavas have remained tholeiitic, with remarkably constant SiO_2 at a given MgO, and do not show evidence of significant decline in melt production accompanied by transition to alkalic and transitional tholeiitic compositions [*Frey and Rhodes*, 1993]. Notable exceptions are the alkalic submarine lavas from two radial vents [*Wanless et al.,* 2006]. The alkalic character of these lavas is due to clinopyroxene fractionation at depth and not a decrease in melt production [*Wanless et al.,* 2006]. Therefore, an alternative explanation is needed for the decline in lava accumulation rate along the submarine rift zone during this protracted period of tholeiitic lava production for > 400 ka. We suggest that sometime between 470 and 300 ka, Mauna Loa evolved from a phase in which both submarine and subearial eruptions took place to one in which effusions were predominantly subaerial. This transition likely took place as the volcano grew in size and elevation because the magma storage zone and attendant rift zones migrated upwards [e.g. *Fiske and Kinoshita,* 1969; *Decker et al.,* 1983] possibly as a consequence of a magma neutral buoyancy zone sandwiched between compacted sub-magma chamber rocks and less-dense overlying lavas [see fig. 33 of *Ryan*, 1987]. A corollary to this interpretation is that Mauna Loa had already attained a significant subaerial structure by 400 to 300 ka.

Even though the eruptive activity along the submarine southwest rift zone decreased over the last several hundred thousand years, it has continued along the subaerial segment of the rift and elsewhere on the volcano during this period. For example, a large embayment in the western flank of Mauna Loa that was created by the South Kona (< 247 ka) and subsequent Alika giant landslides [*Moore et al*., 1994] has been largely filled in by lava flows from the subaerial southwest rift zone. These flows have produced a distinct bulge in the southwest coastline of Hawaii (Figure 1), at a time when eruptive activity on the submarine southwest rift zone was low. Similarly, our data show that the Ninole Basalts were also being erupted on the southeastern flank of the subaerial segment of the rift zone around 230 to 108 ka.

In the absence of several suitably dated sections, it is difficult to obtain reliable quantitative estimates of the rate of Mauna Loa's subaerial eruptive activity [*Lipman*, 1995]. The problem is exacerbated by the fact that even during the tholeitic shield-building stage, eruption rates can wax and wane. This has been shown for recent Mauna Loa [*Lockwood and Lipman*, 1987; *Lockwood*, 1995], Mauna Kea [*Stolper et al*., 2004; *Rhodes et al., 2012*] and Kilauea [*Swanson et al*., 2011]. Data from HSDP-2 indicate a mean lava accumulation rate of ~2.5 mm/yr over the last 120 ka at Mauna Loa on its eastern flank ~40 km from the summit [*Sharp and Renne*, 2005]. The rate, however, has varied significantly during this time from about 1.2 mm/yr to 4.7 mm/yr [*Beeson et al.,* 1996]. Despite the variation, lava accumulation has nearly kept up with subsidence (~2.6 mm/yr) [*Ludwig et al.,* 1991] over the last 120 ka, and exceeds rates typical of post-shield volcanism (< 1mm/yr).

The historical record (1843 – 2012) for Mauna Loa tells a similar story. The total lava output over these 169 years is estimated at ~ 4.1 km^3 [*Lockwood and Lipman*, 1987]. This compares with ~ 6.8 km^3 for Kilauea, the archetypical shield-stage volcano, over this same time period. Mauna Loa's historical lava volume if spread over the entire subaerial volcano (5125 km^2) is sufficient to produce lava accumulation rates of around 5 mm/yr. We argue, therefore, that there is a strong case that Mauna Loa is still in its shield-building stage, albeit focused on the subaerial part of the volcano.

7. Conclusions

Fourteen new $^{40}Ar/^{39}Ar$ age determinations from tholeiitic lavas sampled from the submarine SW flank of Mauna Loa range in age from 657 ± 175 to 59 ± 16 ka. These ages document the eruptive history of Mauna Loa, provide insight into the temporal evolution of the southwest rift zone, and place maximum limits on the ages of the Ka Lae and South Kona debris avalanches. Based on these ages, we offer the following conclusions:

1. Our data indicate maximum ages of around 247 ka for the South Kona landslide, and around 120 ka for the East Ka Lae landslide. Both slides could be much younger.

2. Lavas with Loihi-like isotopic compositions (i.e., high $^{208}Pb/^{204}Pb$ and $^{206}Pb/^{204}Pb$) were erupted along with lavas with isotopic compositions more characteristic of Mauna Loa prior to 250 ka. Lavas with anomalously high $^{208}Pb/^{204}Pb$ relative to $^{206}Pb/^{204}Pb$ were erupted prior to 470 ka, along with lavas with normal isotopic characteristics. Therefore, the plume source of Mauna Loa magmas was more heterogeneous in the past.

3. The two new $^{40}Ar/^{39}Ar$ ages of 227 ± 23 (lava) and 108 ± 35 ka (dike) for the Ninole Basalt overlap with ages for lavas erupted on Mauna Loa's submarine southwest rift zone (~470 to 59 ka). Therefore, the Ninole Basalt is not part of a pre-Mauna Loa volcano or an old Ninole rift zone. These results also show that while eruptive activity on the submarine southwest rift zone had declined dramatically, significant eruptive activity on the subaerial section of the rift zone was taking place.

4. Lava accumulation rates on Mauna Loa’s submarine southwest rift zone were extremely high (~ 25 mm/yr) around 470 ka. This probably reflects the height of the shield-building stage. Between 470 and 273 ka, the lava accumulation rate dropped dramatically to ~1.0 mm/yr and remained at this rate over the next 200 ka. We infer that during this time subaerial eruptive activity was relatively moderate, with lava accumulation rates varying from < 2 mm/yr to about 6 mm/yr. Therefore, we propose that the decline in eruptive activity on the submarine southwest rift zone does not mark the onset of post-shield volcanism, but is, instead, indicative of the evolution of Mauna Loa from a predominantly submarine stage of growth to one that is mainly subaerial. As the volcano has grown in size and elevation, the magma storage zone and attendant rift zones likely have migrated upwards, reducing magma availability to the submarine rift zone.

Acknowledgments. This research was supported by U.S. National Science Foundation grants to Singer (OCE-0825659), Rhodes (OCE-0825787) and Garcia (EAR-0510482). A special thanks to Mike Vollinger for careful preparation of all the samples for geochronology and Darwina Griffin for the production of Figure 1. We also thank Warren Sharp for sharing HSDP-2 samples with us and Anthony Koppers and Pete Lipman for the helpful reviews.

References

Abouchami, W., Hofmann, A. W., Galer, S. J. G., Frey, F., Eisele, J., and M. Feigenson (2005), Long-lived heterogeneities and lateral dichotomy of the Hawaiian plume, *Nature, 434,* 851-856.

Beeson, M. H., Clague, D. A. and Lockwood, J. P. (1996) Origin and depositional environment of clastic deposits in the Hilo drill hole, Hawaii, *J. Geophys. Res. 101,* 11,617-11,629.

Dalrymple, G. B., and J. G. Moore (1968), Argon-40: Excess in submarine pillow basalts from Kilauea, Hawaii, *Science*, *161*, 1132-1135.

Decker, R. W., Koyanagi, R. Y., Dvorak, J. J., Lockwood, J. P., Okamura, A. T., Yamashita, K. M. and Tanigawa, W. R. (1983) Seismicity and surface deformation of Mauna Loa volcano, Hawaii, *Eos*, *64*, 545-547.

DePaolo, D. J., Bryce, J. G., Dodson, A., Shuster, D. A., and B. M. Kennedy (2001), Isotopic evolution of Mauna Loa and the chemical structure of the Hawaiian plume, *Geochem. Geophys. Geosyst.*, *2*, 1044, doi:10.1029/2000GC000139.

DePaolo, D. J., Stolper, E. M., Thomas, D. M., and M. O. Garcia (1999), Hawaiian Scientific Drilling Project: Core Logs and Summarizing Data, vol. 1–4, Calif. Inst. of Technol., Pasadena.

DePaolo, D. J.,and E. M. Stolper (1996), Models of Hawaiian volcano growth and plume structure: Implications of results from the Hawaii Scientific Drilling Project, *J. Geophys Res.*, *101*, 11,643–11,654.

Fiske, R. S. and Kinoshio, W. T. (1969) Inflation of Kilauea Volcano prior to its 1967-1968 eruption, *Science, 165*, 341-349.

Frey, F. A., and J. M. Rhodes (1993), Inter-shield geochemical differences among Hawaiian volcanoes: Implications for source compositions, melting processes and magma ascent paths, *Philos. Trans. R. Soc. London Part A*, *342*, 121–136.

Garcia, M. O., Hulsebosch, T., and J. M. Rhodes (1995), Olivine-rich submarine basalts from the Southwest Rift Zone of Mauna Loa volcano: Implications for magmatic processes and geochemical evolution, in *Mauna Loa Revealed: Structure, Composition, History, and Hazards, Geophys. Monogr. Ser., vol. 92*, edited by J. M. Rhodes and J. P. Lockwood, pp. 219–239, AGU, Washington, D. C.

Garcia, M., Muenow, D., Aggrey, K. and J. O'Neil (1989), Major element, volatile and stable isotope geochemistry of Hawaiian submarine tholeiitic glasses. *J. Geophys. Res.*, *94*, 10,525-10,538.

Garcia, M.O., Haskins, E.H., E. Stolper (2007), Stratigraphy of the Hawaiian Scientific Drilling Project: Anatomy of a Hawaiian volcano. Geochemistry, Geophysics, Geosystems, 8, Q02G20, doi:10.1029/2006GC001379.

Kuiper, K. F., Deino, A., Hilgen, F. J., Krijgsman, W., Renne, P. R., and J. R. Wijbrans (2008) Synchronizing rock clocks of earth history, *Science, 320,* 500-505.

Kurz, M. D., Kenna, T. C., Kammer, D.P., Rhodes, J.M., Garcia, M.O., (1995) Isotopic evolution of Mauna Loa Volcano; a view from the submarine southwest rift zone, in *Mauna Loa Revealed: Structure, Composition,* *History and Hazards, Geophys. Monogr. Ser.,* 92, edited by J. M. Rhodes and J. P. Lockwood, pp. 289-306, AGU, Washington, D. C.

Lipman, P. W. (1995), Declining growth rate of Mauna Loa during the last 100,000 years: Rates of lava accumulation vs gravitational subsidence, in *Mauna Loa Revealed: Structure, Composition, History and Hazards, Geophys. Monogr. Ser.,* 92, edited by J. M. Rhodes and J. P. Lockwood, pp. 45–80, AGU, Washington, D. C.

Lipman, P. W. and Swenson, A. (1984) Generalized geologic map of the southwest tift zone of Mauna Loa Volcano, Hawaii, *U. S. Geol. Surv. Misc. Investig. Map I-1323*, scale1:100,000.

Lipman, P. W., Rhodes, J. M., and G. B. Dalrymple (1990), The Ninole basalt – Implications for the structural evolution of Mauna Loa volcano, Hawaii, *Bull. Volcanol., 53*, 1-19.

Lipman, P. W., Normark, W. R., Moore, J. G., Wilson, J., and C. Gutmacher (1988), The giant submarine 'Ālika debris slide, Mauna Loa, Hawaii, *J. Geophys. Res., 93*, 4279–4299.

Lockwood, J. P. (1995), Mauna Loa eruptive history: The preliminary radiocarbon record, in Mauna Loa Revealed: Structure, Composition, History and Hazards, *Geophys. Monogr. Ser., vol. 92*, edited by J. M. Rhodes and J. P. Lockwood, pp. 45–80, AGU, Washington, D. C.

Lockwood, J. P. and Lipman, P. W. (1987), Holocene eruptive history of Mauna Loa volcano. *U.S. Geol. Surv. Prof. Paper 1350*: 509-535.

Ludwig, K. R., B. J. Szabo, J. G. Moore, and K. R. Simmons (1991), Crustal subsidence rate off Hawaii determined from $^{234}U/^{238}U$ ages of drowned coral reefs, *Geology 19*, 171–174.

Macdonald, G. A., and A. T. Abbott (1970) *Volcanoes in the Sea: The geology of Hawaii*, University of Hawaii Press, Honolulu, 1-441.

Marske, J. P., Pietruszka, A. J., Weis, D., Garcia, M. O. and Rhodes, J. M. (2007) Rapid passage of a small-scale mantle heterogeneity through the melting regions of Kilauea and Mauna Loa volcanoes, *Earth Planet. Sci. Lett. 259*, 34-50.

McMurtry, G. M., Herrero-Bervera, E., Cremer, M. D., Smith, J. R., Resig, J., Sherman, C., and M. E. Torresan (1999), Stratigraphic constraints on the timing and emplacement of the Alika 2 giant Hawaiian submarine landslide, *J. Volcanol. Geotherm. Res., 94*, 35-58.

Min, K., Mundil, R., Renne, P. R., and Ludwig, K. R. (2000), A test for systematic errors in $^{40}Ar/^{39}Ar$ geochronology through comparison with U/Pb analysis of a 1.1-Ga rhyolite, *Geochim. Cosmochim. Acta, 64*, 73-98.

Moore, J.G., and W.W. Chadwick (1995), Offshore geology of Mauna Loa and adjacent area, Hawaii, *Mauna Loa Revealed: Structure, Composition, History and Hazards, Geophys. Monogr. Ser.*, 92, edited by J. M. Rhodes and J. P. Lockwood, pp. 21–44, AGU, Washington, D. C.

Moore, J. G., and D. A. Clague (1992), Volcano growth and evolution of the island of Hawaii, *Geol. Soc. Amer. Bull., 104*, 1471-1484.

Moore, J. G., Clague, D. A., Holcomb, R., Lipman, P., Normark, W., and M. Torresan (1989), Prodigious submarine landslides on the Hawaiian Ridge, *J. Geophys. Res., 94*, 17,465–17,484.

Moore, J. G., Normark, W. R., and B. J. Szabo (1990), Reef growth and volcanism on the submarine southwest rift zone of Mauna Loa, Hawaii, *Bull. Volcanol., 52*, 375-380.

Moore, J. G., W. R. Normark, and R. T. Holcomb (1994), Giant Hawaiian landslides, *Ann. Rev. Earth Planet. Sci.*, *22*, 119-144.

Moore, J. G., Bryan, W. B., Beeson, M. H., and W. R. Normark (1995), Giant blocks in the South Kona landslide, Hawaii, *Geology, 23*, 125-128.

Morgan, J. K., Park, J., and C. A. Zelt (2010), Rift abandonment and reconfiguration in Hawaii: Mauna Loa's Ninole rift zone, *Geology, 38*, 471-474.

Morgan, J. K., Clague, D. A., Borchers, D. C., Davis A. S., and K. L. Milliken (2007), Mauna Loa's submarine western flank: Landsliding, deep volcanic spreading, and hydrothermal alteration, *Geochem. Geophys. Geosyst.*, *8*, Q05002, doi: 10.1029/2006GC001420.

Pringle, M. S. (1993), Age progressive volcanism in the Musicians Seamounts: A test of the Hot Spot Hypothesis for the Late Cretaceous Pacific, in The Mesozoic Pacific: Geology, Tectonics, and Volcanism, *Geophys. Monogr. Ser., vol. 77,* edited by M. S. Pringle et al., pp. 187–216, AGU, Washington, D. C.

Renne, P. R., Cassata, W.S., and L. E. Morgan (2009), The isotopic composition of atmospheric argon and $^{40}Ar/^{39}Ar$ geochronology: Time for a change?, *Quat. Geochronol., 4*, 288–298, doi:10.1016/j.quageo.2009.02.015.

Renne, P. R. (2000) K-Ar and $^{40}Ar/^{39}Ar$ dating. In Noller, J.S., Sowers, J.M., and W.M. Lettis (eds.) , *Quaternary Geochronology: Methods and Applications.* American Geophysical Union reference Shelf 4. Washington, D.C.: American Geophysical Union, pp. 77-100.

Rhodes, J. M., and M. J. Vollinger (2004), Composition of basaltic lavas sampled by phase-2 of the Hawaii Scientific Drilling Project: Geochemical stratigraphy and magma types, *Geochem. Geophys. Geosyst., 5*, Q03G13, doi:10.1029/2002GC000434.

Rhodes, J. M., Huang, S., Frey, F. A., Pringle, M. and Xu, G. (2012) Compositional diversity of Mauna Kea shield lavas recovered by the Hawaii Scientific Drilling Project: Inferences on source lithology, magma supply, and the role of multiple volcanoes, *Geochem. Geophys. Geosyst.*, *13*, Q03013, doi:10.1029/2011GC003812.

Ryan. M. P. (1987) Elasticity and contractancy of Hawaiian olivine tholeiite and its role in the stability and structural evolution of subcaldera magm reservoirs and rift systems, *U.S. Geol. Surv. Prof. Paper 1350*: 1395-1447.

Sharp, W. D., B. D. Turrin, P. R. Renne, and M. A. Lanphere (1996), The $^{40}Ar/^{39}Ar$ and K/Ar dating of lavas from the Hilo 1-km core hole, Hawaii Scientific Drilling Project, *J. Geophys. Res., 101*, 11,607–11,616.

Sharp, W. D., and P. R. Renne (2005), The $^{40}Ar/^{39}Ar$ dating of core recovered by the Hawaii Scientific Drilling Project (phase 2), Hilo, Hawaii, *Geochem. Geophys. Geosyst., 6*, Q04G17, doi: 10.1029/2004GC000846.

Staudigel, H., Plank, T., White, W., and H.-U. Schmincke (1996), Geochemical fluxes during seafloor alteration of basaltic upper oceanic crust: DSDP sites 417 and 418, in Subduction Top to Bottom, *Geophys. Monogr. Ser., vol. 96*, edited by G. E. Bebout et al., pp. 19–38, AGU, Washington, D. C.

Stearns, H. T., and W. O. Clark (1930) Geology and water resources of the Kau district, Hawaii, *U.S. Geol. Surv. Water-Supply paper, 616*, 1-94.

Steiger, R. H., and E. Jäger (1977), Subcommission on geochronology; convention on the use of decay constants in geo-and cosmochronology, *Earth Planet. Sci. Lett. 36*, 359-362.

Stolper, E., DePaolo, D. J. and Thomas, D. M. (1996) The Hawaii Scientific Drilling Project: introduction to the special section, *J. Geophys. Res. 101*, 11593-11598.

Stolper, E., Sherman, S., Garcia, M., Baker, M., and C. Seaman (2004), Glass in the submarine section of the HSDP2 drill core, Hilo, Hawaii, *Geochem. Geophys. Geosyst., 5*, Q07G15, doi:10.1029/2003GC000553.

Swanson, D.A., Rose, T.A., Mucek, A.E., Garcia, M.O., Fiske, R.S., and L.G. Mastin (2011), A Different View of Kilauea's Past 2500 Years, Abstract V33E-07, presented at 2011 Fall Meeting, AGU, San Francisco, Calif., 5-9 Dec.

Trusdell, F. A. & Lockwood, J. P. Geologic Maps of the Northeast Flank of, Central-Southeast Flank of, Southern Mauna Loa Volcano, Island of Hawai'i, Hawai'i: US Geological Survey SIM 2932-A, SIM 2932-B, SIM 2932-C respectively, scale 1:50,000 (in the press).

Wanless, V. D., Garcia, M. O., Rhodes, J. M., Weis, D., and M. D. Norman (2006), Shield stage alkali volcanism on Mauna Loa volcano, Hawaii, *J. Volcanol. Geotherm. Res.*, 151, 141-155.

Webster, J. M., Clague, D. A., Riker-Coleman, K., Gallup, C., Braga, J. C., Potts, D., Moore, J. G., Winterer, E. L., and C. K. Paull (2004), Drowning of the -150 m reef off Hawaii: A casualty of global meltwater pulse 1A, *Geology, 32*, 249-252.

Weis, D., Garcia, M.O., Rhodes, J.M., Jellinek, M.,and J.S. Scoates (2011), Role of the deep mantle in generating the compositional asymmetry of the Hawaiian mantle plume, *Nature Geoscience,* 4, 831-838.

Wolf, E. W. and Morris, J. (1996) Geologic map of the island of Hawaii, *U.S. Geol. Surv. Misc. Investig. Map I-2524-A*, scale 1:100,000.

Wright, T.L. (1971) Chemistry of Kilauea and Mauna Loa lava in space and time, *United States Geol. Surv. Professional Paper 735,* 40 p.

FIGURE CAPTIONS

Figure 1. Map of southern tip of Hawaii and southwest rift zone showing the locations of the JASON-2, PISCES V dives, and dredges. Bathymetry is from the TN151 cruise (2002) and hillshade basemap is modified from *Wanless et al.* [2006]. Resolution is ~180 m for basemap and ~ 27m for TN151 data. Map is projected in North American 1983 UTM Zone 5 datum.

Figure 2. The $^{40}Ar/^{39}Ar$ age spectra and isochrons for samples SR0413-4.0 and SR781-21.2 from HSDP-2, which were previously $^{40}Ar/^{39}Ar$-dated by *Sharp and Renne* [2005]. Ages of each

experiment are shown with the 2σ uncertainties. Uncertainties of the weighted mean ages are at the 95% confidence interval. Filled ellipses are included in isochron regression; unfilled are not.

Figure 3. Cross-section of southwest rift zone of Mauna Loa showing locations of 14-15 ka coral reef, 130 ka boulder field, sample locations, and dated samples. Dashed lines represent age contours. Dotted line represents top of the landslide scarp section. Observations during Pisces dive 183 noted a conglomerate unit with large (up to 5 m in diameter) boulders, indicative of an older shoreline, "perched" at the top of the landslide scarp at a depth of 425 mbsl [*Garcia et al.*, 1995]. These boulders were undoubtedly present before the landslide. Sea level subsidence curves [*Moore et al.*, 1990], suggest an age of ~130 ka for this shoreline. U-series dating indicates that the reef was drowned at ~14-15 ka [*Moore et al.,* 1990; *Webster et al.,* 2004].

Figure 4. The $^{40}Ar/^{39}Ar$ age spectrum and isochron for J2-16-04, which is located near the base of the submarine southwest rift zone section exposed by the Ka Lae landslide (2112 mbsl).

Figure 5. The $^{40}Ar/^{39}Ar$ age spectrum and isochron for a tholeiite sample J2-20-14 from Mauna Loa's southwest rift zone (857 mbsl). Uncertainties and symbols as in Figure 2.

Figure 6. The $^{40}Ar/^{39}Ar$ age spectrum and isochron for J2-20-20, which is located near the top of the submarine southwest rift zone section exposed by the Ka Lae landslide (600 mbsl). Uncertainties and symbols as in Figure 2.

Figure 7. The $^{40}Ar/^{39}Ar$ age spectrum and isochron for J2-20-22 (501 mbsl). Uncertainties and symbols as in Figure 2.

Figure 8. The $^{40}Ar/^{39}Ar$ age spectrum and isochron for surface flow J2-24-01 located below the southwest rift zone (4537 mbsl). Uncertainties and symbols as in Figure 2.

Figure 9. The $^{40}Ar/^{39}Ar$ age spectrum and isochron for a basalt from the South Kona debris avalanche (3700 mbsl). Uncertainties and symbols as in Figure 2.

Figure 10. The $^{40}Ar/^{39}Ar$ age spectra and isochrons for a dike (SW-77) and basaltic lava (SW-45) from the subaerial Ninole hills. Small upward arrow indicates the presence of a single heating step with an age >1500 ka. Uncertainties and symbols as in Figure 2.

Figure 11. Relationship of high-precision $^{208}Pb/^{204}Pb$ versus $^{206}Pb/^{204}Pb$ for Mauna Loa lavas with inferred age based on stratigraphic relationship to successfully dated samples (Table 1). The samples have been subdivided into three broad age categories. Less than 240 ka (open triangle); between 240 and 470 ka (open square); and greater than 470 ka (filled diamond). The solid line separating the trends for Loa and Kea volcanoes is from Abouchami et al. [2005]. Mauna Loa isotopic data are from *Abouchami et al*. [2005], *Wanless et al*. [2006], *Marske et al*. [2007], *Weis et al*. [2011]. Data for Loihi field from *Abouchami et al*. [2005].

Figure 12. Depth-age relations for Mauna Loa's southwest rift zone and HSDP-2 core shown as depth in section (m) vs. age (ka). Weighted mean $^{40}Ar/^{39}Ar$ plateau ages from this study are

shown with uncertainties at 95% confidence interval. Mauna Loa accumulation rate model of *DePaolo et al*. [2001] and Mauna Kea model of *Sharp and Renne* [2005] are shown for comparison.

Table 1. Summary of $^{40}Ar/^{39}Ar$ experiments

	Depth	Depth in	K/Ca	Total fusion		Isochron				Plateau
Sample #	mbsl	section (m)	total	Age (ka) ± 2σ	$^{40}Ar/^{36}Ar_i$ ± 2σ	Age (ka) ± 2σ	N	^{39}Ar %	MSWD	Age (ka) ± 2σ
Southwest rift zone										
J2-20-22	501		0.07	62 ± 33	297.0 ± 9.4	41 ± 52	6 of 8	98.9	0.33	55 ± 24
			0.08	80 ± 39	295.6 ± 9.7	61 ± 54	6 of 8	99.2	0.35	62 ± 23
					Weighted mean plateau age from 2 experiments:					**59 ± 16**
184-13	550	0	0.06	240 ± 87	297.6 ± 20.3	42 ± 94	7 of 8	69.3	0.14	104 ± 85
			0.05	313 ± 72	296.6 ± 8.1	95 ± 175	7 of 9	67.6	0.10	126 ± 51
					Weighted mean plateau age from 2 experiments:					**120 ± 43**
J2-20-20	600	110	0.14	230 ± 68	298.3 ± 27.4	175 ± 179	11 of 12	99.6	0.31	221 ± 48
			0.15	185 ± 27	300.9 ± 7.1	109 ± 57	15 of 15	100.0	0.87	185 ± 23
			0.14	199 ± 24	297.9 ± 5.5	169 ± 59	14 of 14	100.0	0.67	198 ± 16
					Weighted mean plateau age from 3 experiments:					**196 ± 12**
J2-20-17	668	178	0.03	362 ± 114	297.7 ± 2.5	236 ± 72	7 of 7	100.0	0.92	313 ± 93
			0.03	262 ± 143	296.6 ± 2.5	217 ± 71	7 of 7	100.0	0.45	252 ± 68
					Weighted mean plateau age from 2 experiments:					**273 ± 55**
J2-20-14	857	367	0.09	496 ± 97	303.3 ± 22.1	253 ± 366	8 of 12	84.8	0.23	450 ± 83
			0.12	629 ± 33	308.1 ± 21.4	295 ± 251	6 of 10	76.2	0.63	477 ± 29
					Weighted mean plateau age from 2 experiments:					**474 ± 27**
184-8	1020	470	0.07	512 ± 148	296.4 ± 4.5	382 ± 306	11 of 13	95.0	0.12	449 ± 110
			0.03	475 ± 64	296.3 ± 8.3	456 ± 160	8 of 8	100.0	0.54	472 ± 55
			0.04	451 ± 56	293.0 ± 6.2	515 ± 159	7 of 8	99.4	0.34	453 ± 56
					Weighted mean plateau age from 3 experiments:					**461 ± 36**
183-4	1075	650	0.10	433 ± 84	296.6 ± 6.2	374 ± 352	10 of 13	94.7	0.22	458 ± 82
			0.05	487 ± 83	294.8 ± 3.2	495 ± 108	8 of 8	100.0	0.21	476 ± 62
			0.06	448 ± 73	296.5 ± 3.7	432 ± 135	7 of 8	97.3	0.53	465 ± 62
					Weighted mean plateau age from 3 experiments:					**468 ± 38**
J2-19-10	1753	1263	0.10	466 ± 65	295.7 ± 5.2	470 ± 126	14 of 15	98.2	0.24	473 ± 49
			0.10	520 ± 79	296.2 ± 4.8	437 ± 123	14 of 16	93.9	0.11	454 ± 50
			0.04	491 ± 126	296.4 ± 3.6	435 ± 168	6 of 7	98.5	0.19	470 ± 83
			0.05	576 ± 125	295.5 ± 3.9	464 ± 175	6 of 7	93.5	0.08	463 ± 75
			0.03	470 ± 170	295.6 ± 5.3	442 ± 227	9 of 10	98.1	0.39	445 ± 103
					Weighted mean plateau age from 5 experiments:					**463 ± 28**
J2-16-04	2112	1622	0.04	466 ± 144	295.7 ± 3.2	460 ± 197	8 of 10	95.7	0.17	473 ± 107
			0.05	500 ± 207	297.3 ± 10.9	387 ± 397	8 of 8	100.0	0.14	458 ± 148
			0.05	528 ± 190	294.7 ± 12.5	510 ± 398	6 of 8	90.1	0.45	479 ± 157
					Weighted mean plateau age from 3 experiments:					**470 ± 74**
Surface flows below southwest rift zone										
J2-24-14	3963		0.02	471 ± 328	292.2 ± 18.5	735 ± 743	7 of 8	96.6	0.37	538 ± 208
			0.02	673 ± 355	300.3 ± 15.9	232 ± 345	7 of 7	100.0	0.33	550 ± 219
					Weighted mean plateau age from 2 experiments:					**543 ± 150**
J2-24-01	4537		0.04	836 ± 270	297.6 ± 3.7	589 ± 445	8 of 8	100.0	0.46	856 ± 210
			0.07	709 ± 192	295.3 ± 5.1	650 ± 296	7 of 8	97.4	0.02	637 ± 108
						657 ± 175				683 ± 96
South Kona landslide deposit										
M1203	3700		0.04	384 ± 75	301.6 ± 18.7	185 ± 147	6 of 9	87.2	0.62	**247 ± 56**

Table 1. continued

Sample #	Depth mbsl	Depth in section (m)	K/Ca total	Total fusion Age (ka) ± 2σ	Isochron $^{40}Ar/^{36}Ar_i$ ± 2σ	Isochron Age (ka) ± 2σ	N	^{39}Ar %	MSWD	Plateau Age (ka) ± 2σ
Ninole Hills										
SW-77			0.06	404 ± 93	296.1 ± 1.5	81 ± 77	7 of 8	86.9	0.41	111 ± 68
lava			0.06	482 ± 100	296.1 ± 1.3	87 ± 56	6 of 8	87.0	0.33	107 ± 41
					Weighted mean plateau age from 2 experiments:					**108 ± 35**
SW-45			0.09	204 ± 48	291.2 ± 9.3	230 ± 55	8 of 8	100.0	0.59	211 ± 38
dike			0.09	236 ± 39	294.2 ± 4.4	244 ± 36	8 of 9	99.3	0.23	237 ± 29
					Weighted mean plateau age from 2 experiments:					**227 ± 23**
Hawaii Scientic Drilling Project (HSDP-2) drill core samples										
SR413-4.0	984.2		0.03	330 ± 147	295.8 ± 6.4	313 ± 378	6 of 8	95.5	0.06	332 ± 134
			0.02	371 ± 135	295.2 ± 6.9	413 ± 368	7 of 9	95.8	0.11	396 ± 134
					Weighted mean plateau age from 2 experiments:					**364 ± 93**
SR781-21.2	2242		0.03	522 ± 157	297.5 ± 5.4	363 ± 312	6 of 7	98.4	0.19	477 ± 109
			0.03	492 ± 145	296.5 ± 5.9	449 ± 283	6 of 8	93.0	0.26	499 ± 107
					Weighted mean plateau age from 2 experiments:					**488 ± 75**

Ages calculated relative to 28.201 Ma for the Fish Canyon sanidine [*Kuiper et al.,* 2008] using decay constants of *Min et al.* [2000]
Age in **bold** is preferred
All uncertainties reflect 2σ analytical uncertainties(including J uncertainty) except for weighted mean ages which are at the 95% confidence level

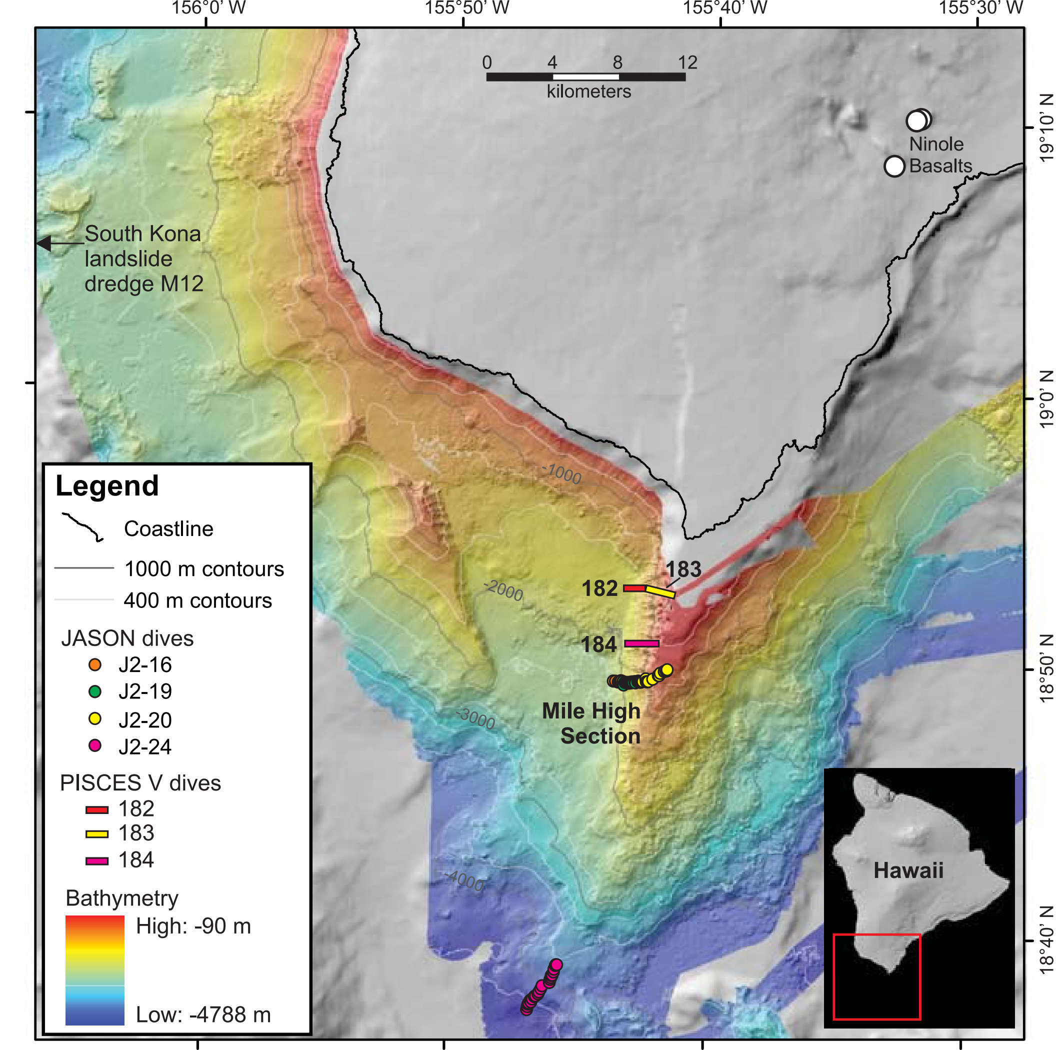
156°0' W
155°50' W
155°40' W
155°30' W
19°10' N
19°0' N
18°50' N
18°40' N
0
4
8
12
kilometers
Ninole
Basalts
South Kona
landslide
dredge M12
-1000
-2000
-3000
-4000
182
183
184
Mile High
Section
Hawaii
Legend
Coastline
1000 m contours
400 m contours
JASON dives
J2-16
J2-19
J2-20
J2-24
PISCES V dives
182
183
184
Bathymetry
High: -90 m
Low: -4788 m

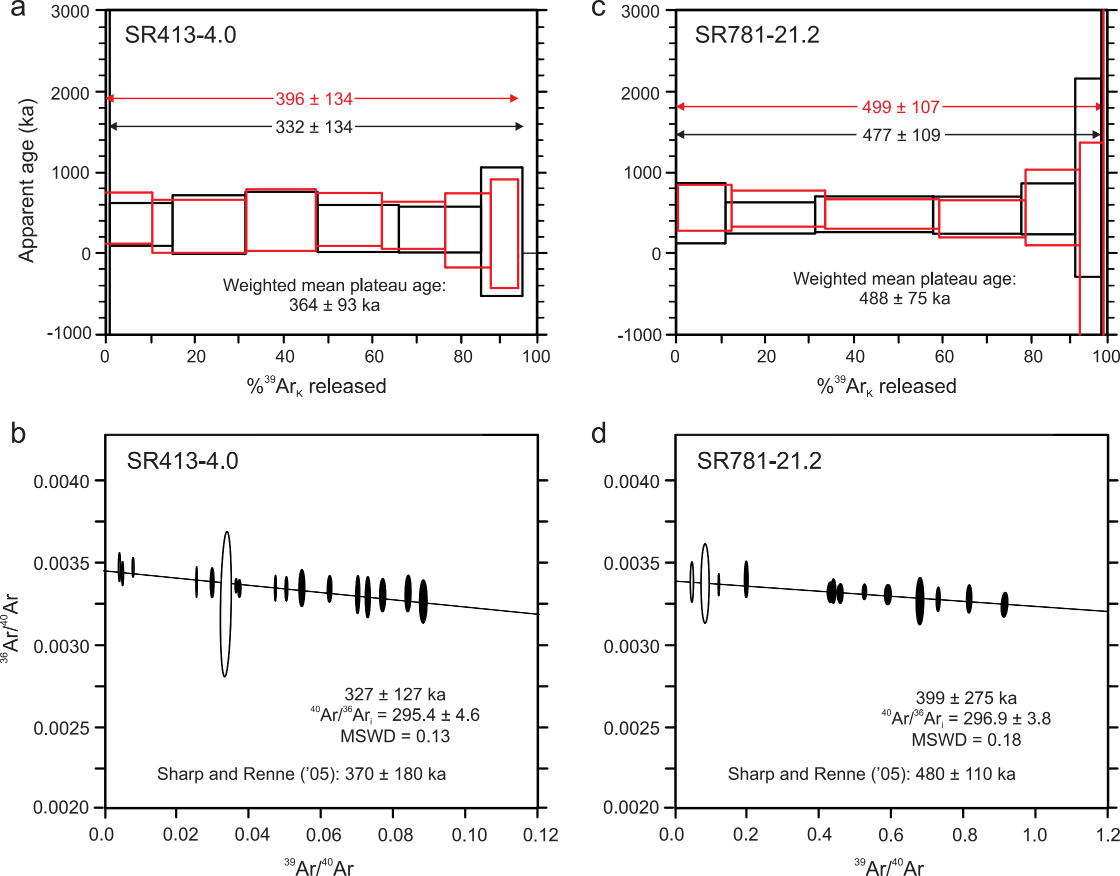

a
SR413-4.0
Apparent age (ka)
396 ± 134
332 ± 134
Weighted mean plateau age:
364 ± 93 ka
% $^{39}Ar_K$ released
c
SR781-21.2
499 ± 107
477 ± 109
Weighted mean plateau age:
488 ± 75 ka
% $^{39}Ar_K$ released
b
SR413-4.0
$^{36}Ar/^{40}Ar$
327 ± 127 ka
$^{40}Ar/^{36}Ar_i$ = 295.4 ± 4.6
MSWD = 0.13
Sharp and Renne ('05): 370 ± 180 ka
$^{39}Ar/^{40}Ar$
d
SR781-21.2
399 ± 275 ka
$^{40}Ar/^{36}Ar_i$ = 296.9 ± 3.8
MSWD = 0.18
Sharp and Renne ('05): 480 ± 110 ka
$^{39}Ar/^{40}Ar$

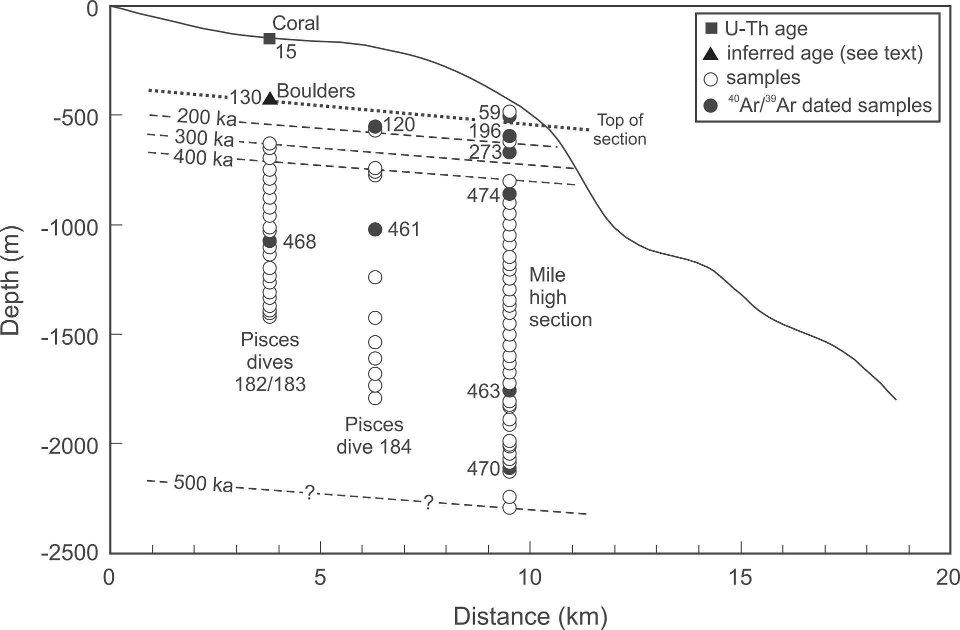
U-Th age
inferred age (see text)
samples
$^{40}Ar/^{39}Ar$ dated samples
Coral
15
130
Boulders
200 ka
300 ka
400 ka
500 ka
?
?
Top of section
59
196
273
474
463
470
120
461
468
Pisces dives 182/183
Pisces dive 184
Mile high section
Depth (m)
Distance (km)
0
-500
-1000
-1500
-2000
-2500
0
5
10
15
20

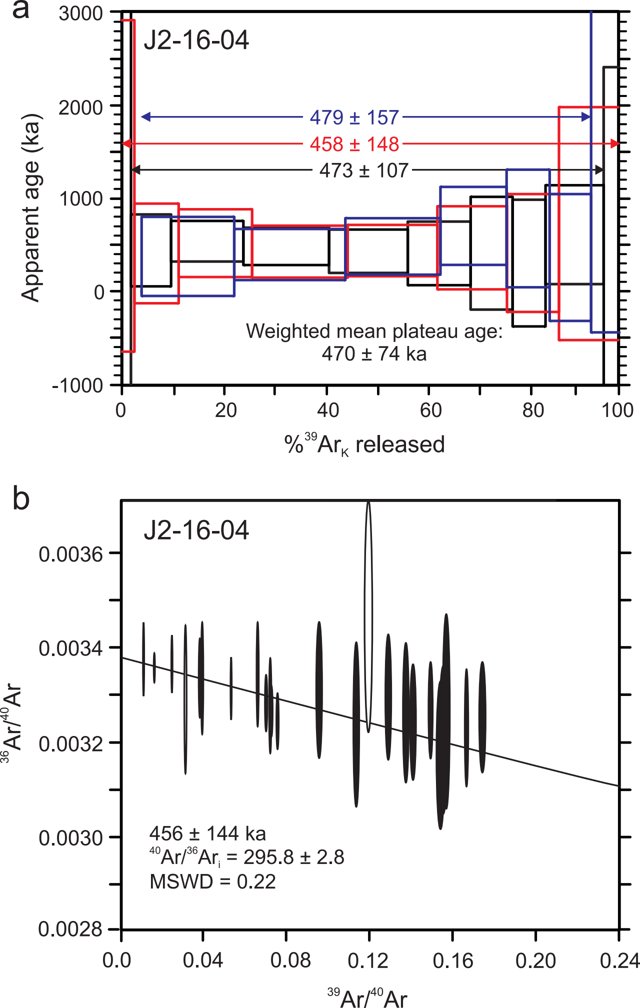
a
J2-16-04
Apparent age (ka)
3000
2000
1000
0
-1000
479 ± 157
458 ± 148
473 ± 107
Weighted mean plateau age:
470 ± 74 ka
0
20
40
60
80
100
% $^{39}Ar_K$ released
b
J2-16-04
$^{36}Ar/^{40}Ar$
0.0036
0.0034
0.0032
0.0030
0.0028
456 ± 144 ka
$^{40}Ar/^{36}Ar_i$ = 295.8 ± 2.8
MSWD = 0.22
0.0
0.04
0.08
0.12
0.16
0.20
0.24
$^{39}Ar/^{40}Ar$

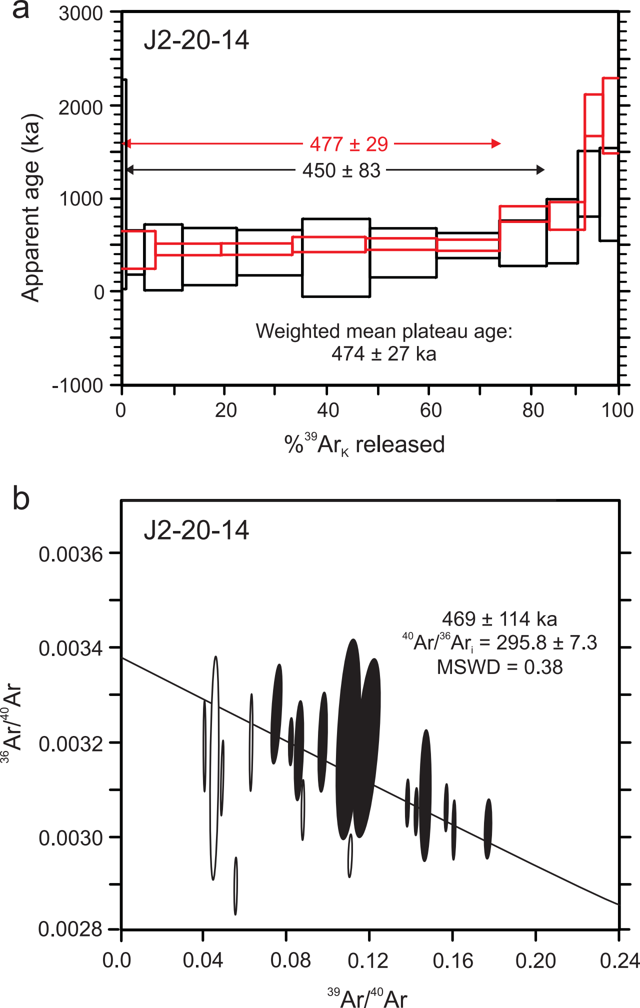
a
J2-20-14
Apparent age (ka)
3000
2000
1000
0
-1000
477 ± 29
450 ± 83
Weighted mean plateau age:
474 ± 27 ka
0
20
40
60
80
100
% $^{39}Ar_K$ released
b
J2-20-14
0.0036
0.0034
0.0032
0.0030
0.0028
$^{36}Ar/^{40}Ar$
469 ± 114 ka
$^{40}Ar/^{36}Ar_i$ = 295.8 ± 7.3
MSWD = 0.38
0.0
0.04
0.08
0.12
0.16
0.20
0.24
$^{39}Ar/^{40}Ar$

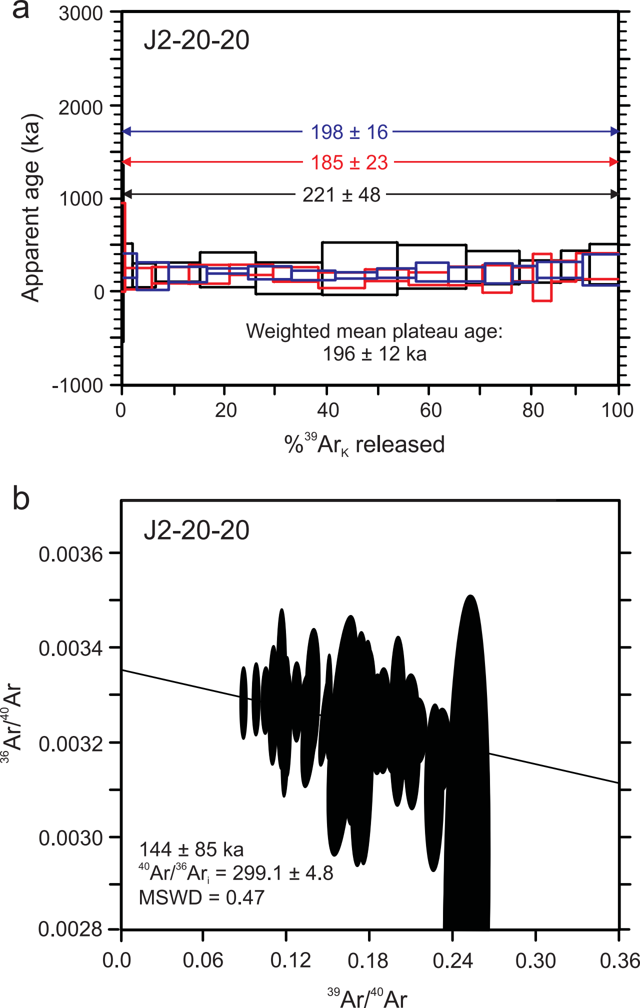
a
J2-20-20
Apparent age (ka)
3000
2000
1000
0
-1000
198 ± 16
185 ± 23
221 ± 48
Weighted mean plateau age:
196 ± 12 ka
0
20
40
60
80
100
% $^{39}Ar_K$ released
b
J2-20-20
0.0036
0.0034
0.0032
0.0030
0.0028
$^{36}Ar/^{40}Ar$
144 ± 85 ka
$^{40}Ar/^{36}Ar_i$ = 299.1 ± 4.8
MSWD = 0.47
0.0
0.06
0.12
0.18
0.24
0.30
0.36
$^{39}Ar/^{40}Ar$

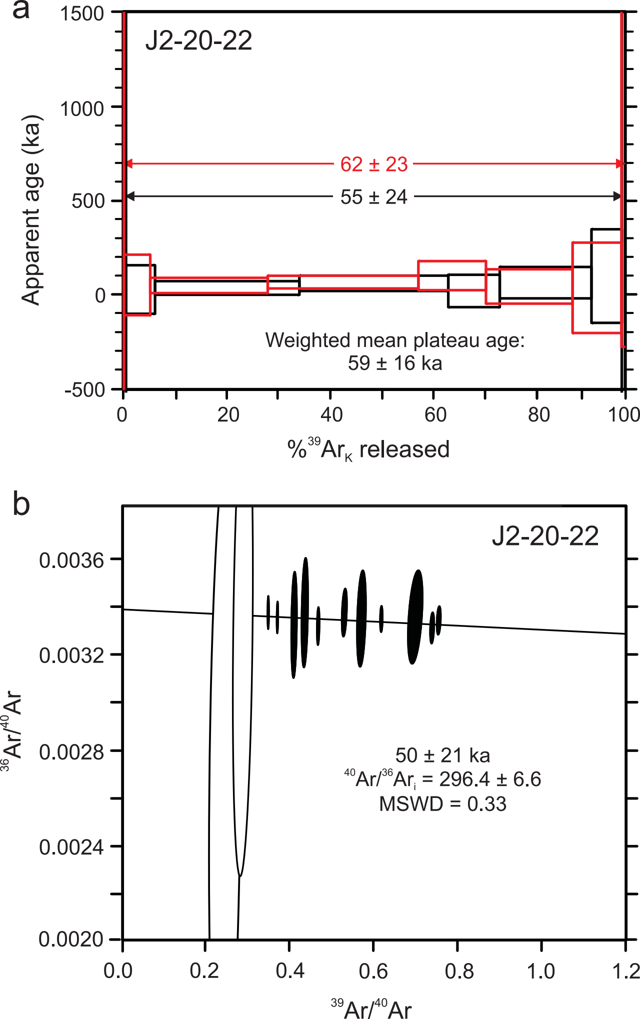

a
J2-20-22
62 ± 23
55 ± 24
Weighted mean plateau age:
59 ± 16 ka
Apparent age (ka)
1500
1000
500
0
-500
0
20
40
60
80
100
%39ArK released
b
J2-20-22
50 ± 21 ka
40Ar/36Ari = 296.4 ± 6.6
MSWD = 0.33
36Ar/40Ar
0.0036
0.0032
0.0028
0.0024
0.0020
0.0
0.2
0.4
0.6
0.8
1.0
1.2
39Ar/40Ar

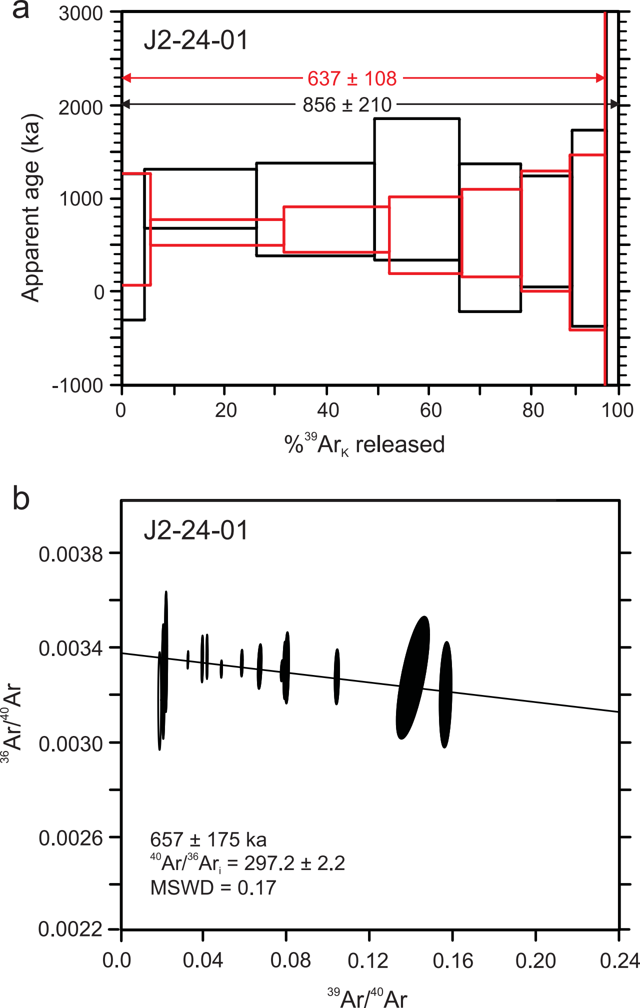

a
J2-24-01
637 ± 108
856 ± 210
Apparent age (ka)
3000
2000
1000
0
-1000
0
20
40
60
80
100
% 39ArK released
b
J2-24-01
0.0038
0.0034
0.0030
0.0026
0.0022
36Ar/40Ar
657 ± 175 ka
40Ar/36Ari = 297.2 ± 2.2
MSWD = 0.17
0.0
0.04
0.08
0.12
0.16
0.20
0.24
39Ar/40Ar

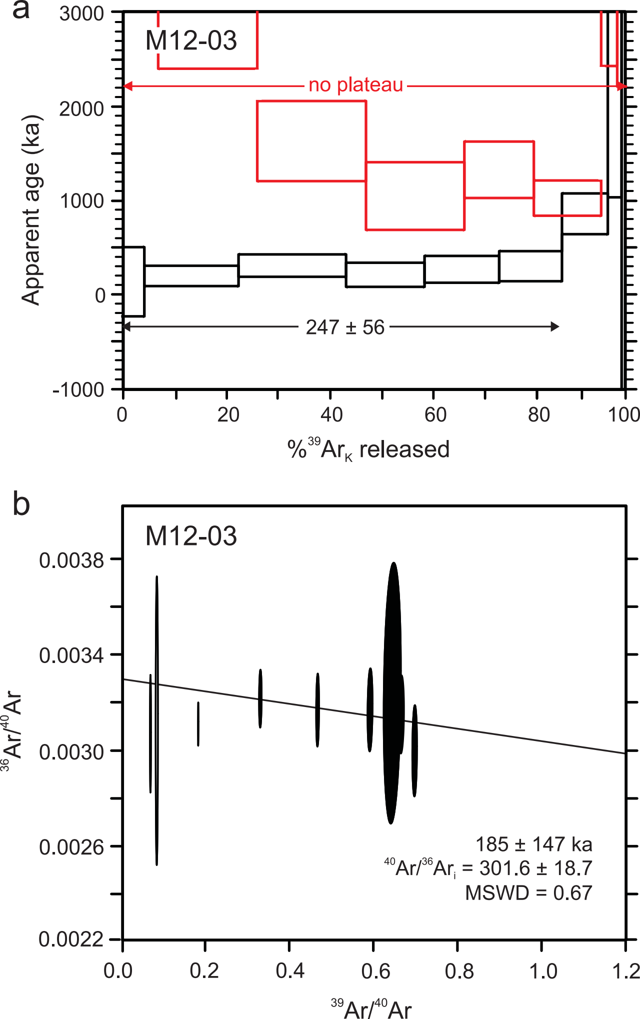
a
M12-03
no plateau
247 ± 56
Apparent age (ka)
3000
2000
1000
0
-1000
0
20
40
60
80
100
%$^{39}Ar_K$ released
b
M12-03
185 ± 147 ka
$^{40}Ar/^{36}Ar_i$ = 301.6 ± 18.7
MSWD = 0.67
$^{36}Ar/^{40}Ar$
0.0038
0.0034
0.0030
0.0026
0.0022
0.0
0.2
0.4
0.6
0.8
1.0
1.2
$^{39}Ar/^{40}Ar$

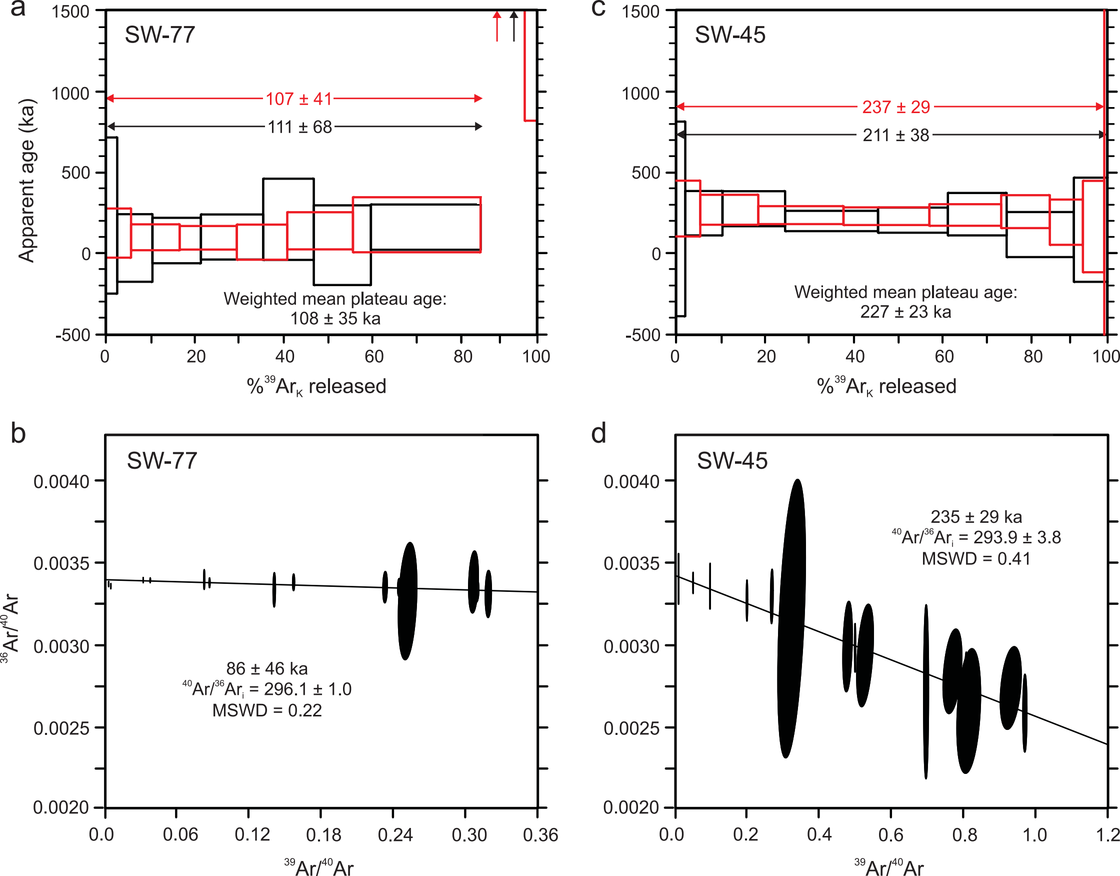
a
SW-77
107 ± 41
111 ± 68
Weighted mean plateau age:
108 ± 35 ka
Apparent age (ka)
%$^{39}Ar_K$ released
c
SW-45
237 ± 29
211 ± 38
Weighted mean plateau age:
227 ± 23 ka
%$^{39}Ar_K$ released
b
SW-77
86 ± 46 ka
$^{40}Ar/^{36}Ar_i$ = 296.1 ± 1.0
MSWD = 0.22
$^{36}Ar/^{40}Ar$
$^{39}Ar/^{40}Ar$
d
SW-45
235 ± 29 ka
$^{40}Ar/^{36}Ar_i$ = 293.9 ± 3.8
MSWD = 0.41
$^{39}Ar/^{40}Ar$

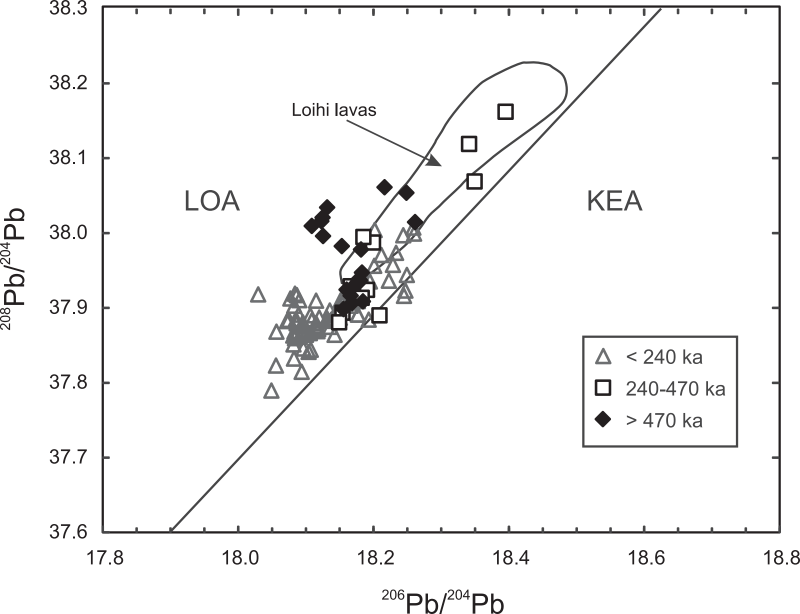

38.3
38.2
38.1
38.0
37.9
37.8
37.7
37.6
17.8
18.0
18.2
18.4
18.6
18.8
$^{208}Pb/^{204}Pb$
$^{206}Pb/^{204}Pb$
Loihi lavas
LOA
KEA
< 240 ka
240-470 ka
> 470 ka

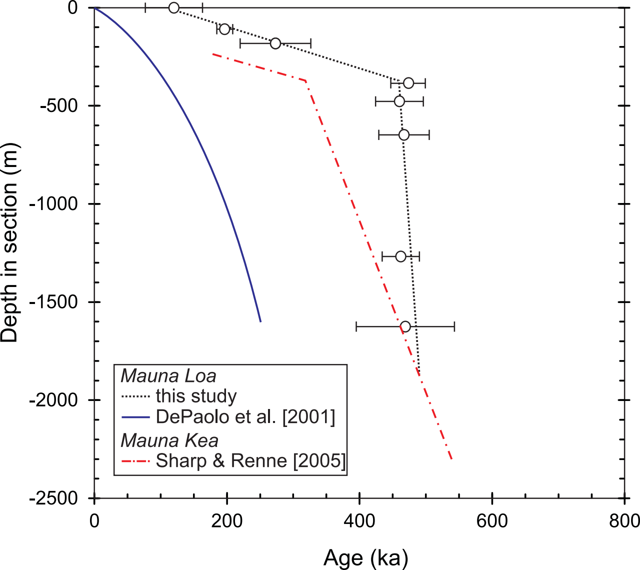

0
-500
-1000
-1500
-2000
-2500
Depth in section (m)
0
200
400
600
800
Age (ka)
Mauna Loa
this study
DePaolo et al. [2001]
Mauna Kea
Sharp & Renne [2005]